PAPER

Check for updates

Zeolites as sustainable alternatives to traditional tanning chemistries†

William R. Wise, [ID] [a] Stefan J. Davis, [ID] *[a] Wouter E. Hendriksen, [ID] [b] Dirick J. A. von Behr, [b] Sujay Prabakar [ID] [c] and Yi Zhang [ID] [c]

Collagen-based composite materials are extensively studied and used in different fields, including tissue engineering, food applications and leather manufacture. Leather is the largest application of collagen where typical tanning chemistries include metal salts, polyphenolics and aldehydes. A new type of material that is gaining industrial significance is based on a composite of collagen and zeolite in the area of sustainable leather manufacture. This approach utilises simple, abundant, and benign chemistry, which provides leather with the physical properties needed for a range of possible applications. However, the stabilising interactions between collagen and zeolite are not yet known and would benefit from deeper understanding of the interactions and the impact on environmental parameters. The composite material reported here is made by treating animal hide collagen with zeolite using established processing technologies, commonly used in leather tanning processes, without the need for further specialised apparatus. The interaction between collagen and zeolite has been characterised by small-angle X-ray scattering (SAXS), infrared spectroscopy (IR), solid-state nuclear magnetic resonance spectroscopy (NMR), scanning electron microscopy (SEM) and zeta potential. SAXS shows unique changes in the scattering profile revealing zeolite and collagen interactions, which relate to a combination of covalent and electrostatic mechanisms. The zeolite forms a 3D network structure covering collagen fibres, improving protein stability against hydrothermal denaturation and creating material strength. The environmental and industrial impact has been evaluated based on reaction uptake, waste stream assessment and biodegradability. Zeolite tanning shows a positive influence on reaction uptakes, similar to industry best practice, waste water impact and positive biodegradability results. Through the deeper understanding of the van der Waals interactions between collagen and zeolite, and the positive environmental assessment, this work demonstrates the merits of this new stabilisation approach with the possibility of further expansion into other applications.

Introduction

Collagen is an abundant protein with a range of sources and a variety of possible applications, however, it is susceptible to putrefaction caused by bacteria, and stabilisation imparting long-term preservation is required.[1] As well as a preservative measure, the stabilisation effect can facilitate other changes in material properties including: softness, a transition from translucency to opacity and a colour characteristic of the agent used.[1] A significant increase in the material resistance to denaturation from heat under high humidity conditions is also observed.[2,3] During denaturation, the hydrogen-bonding network within the collagen structure is disrupted which allows a transition from a helical to a random coil structure.[4,5] The denaturation of collagen has been shown to be an endothermic process coupled with an increase in system entropy, and when chemically stabilised, the thermodynamics are affected as a consequence.[4,5] Ideally, the chemistry employed to stabilise a substrate would lower the system entropy and increase the endothermic enthalpy requirements of the denaturing process. Mineral stabilising agents utilising chromium(III) have been shown to significantly increase the endothermic enthalpy requirements of the denaturing process, whereas all other stabilising agents (mineral, plant extract or synthetic) denature through entropically controlled processes.[1,5]

Leather is the single biggest use of collagen biomaterials, which accounts for in excess of 20 million cattle hides being

[a]Institute for Creative Leather Technologies, The University of Northampton, University Drive, Northampton, NN15PH, UK.
E-mail: stefan.davis@northampton.ac.uk
[b]Smit & Zoon, Nijverheidslaan 48, 1382LK Weesp, The Netherlands
[c]Leather and Shoe Research Association of New Zealand, Palmerston North, New Zealand
†Electronic supplementary information (ESI) available. See DOI: https://doi.org/10.1039/d3gc00381g

processed per annum.[6] Historically, plant extracts were used to stabilise animal hides against putrefaction until the end of the nineteenth century.[1] The use of chromium(III) salts as stabilising agents first adopted commercially in 1884.[7,8] Chromium (III) salts are the most common stabilising agents, and are utilised by over 80% of the global leather industry.[8] Despite chromium(III) salts providing industrially effective stabilising agents, there are growing concerns regarding the environmental and health impacts of the use of chromium(III) stabilising agents. Uncertainty in the concentration of chromium(VI) in chromium(III)-tanned leather, and the public misconception that chromium(III) biochemistry is equivalent to that of chromium(VI), are directing end-users towards chromium-free leather.[8] These problems are not helped by the possibility of chromium(VI) being formed as a contaminant due to oxidation of chromium(III) under ambient conditions, or by the presence of oxidising organics.[9,10] Issues associated with chromium(III) supply and the recycling of chromium(III) – tanned leather, have necessitated research for a suitable alternative stabilising agent which ideally confers similar properties to chromium(III) tanning salts.[11]

Zeolites are aluminosilicate frameworks with cations from group I or II trapped in tunnels of cages, which allows these materials to exchange ions for those present in the surrounding solvent.[12] The preparation of synthetic zeolites typically involves the heating of colloidal silica to 100–200 °C within an autoclave in the presence of (in)organic hydroxides as templating components and high surface area alumina, which provide nucleation sizes of a defined size.[12] The resulting microcrystalline aluminosilicates are heated to 500 °C to burn away the organic components.[12] Zeolites are commonly characterised by the aluminium–silicon ratio and by the presence of the small cations used to maintain charge neutrality.[12] In type-A zeolites, the aluminium–silicon ratio is 1 : 1 and the charge imbalance is neutralised by the presence of Na^+ ions to give the general formula $Na_{12}(AlO_2)_{12}(SiO_2)_{12} \cdot xH_2O$.[12] Although zeolites can be manufactured or found in nature, the starting components are highly abundant in the earth crust and readily accessible.[13] Given the origins of the zeolite components and the benign characteristics, there is potential for applications of zeolites to improve the circular economic credentials of a process or product. In addition to industrially useful availability, zeolites are non-toxic and suitable for veterinary and human use.[14]

The zeolite-collagen composites are a current topic in tissue engineering and bone regeneration.[15,16] Zeolites have long been established as detergents for the laundry industry.[17] The application of water soluble silicates (wasserglass) in leather production to improve dimensional stability during mechanical processing has been previously reported.[18] Previous work relating to the leather sector has indicated zeolite derivatives have potential to stabilise leather materials, which was dependent on the extent, and method, of the breakdown of the silicate structure.[19–21] These previous works focused on the application but lacked the characterisation and mechanistic understanding required to fully utilise this chemistry for industrial

use. The collagen-stabilising potential of zeolites has recently been introduced as an industrial alternative to established chemistries, which has prompted the need to study the green metrics of this approach. The novelty of this study is in providing a deeper insight into the characterisation and mechanism of zeolite tanning of animal hide collagen. Furthermore, a comparison of the green metrics of this tanning chemistry is made to industrial best practices.

Methods

Materials

The commercial zeolite product was supplied by Nera (Netherlands) with the name of Zeology – MZ 8132 and used as received. In brief, the zeolite is based on a compound of aluminium, silicon and oxygen, combined with carboxylic acids, as described elsewhere.[21,22] Bovine hides and limed pelts were purchased from industry sources and treated according to standard industrial processes.

Zeolite-tanned leather material production

Fresh cattle hides, Heavy Texas Steer, were processed based on standard beamhouse operations, up to the state of alkaline-swelling (known as liming). The hides were split to 2.7–2.9 mm and weighed, after which they were delimed according to standard industry practices. The hides were then tanned with the zeolite containing commercial product, Zeology – MZ 8132. The applied amount was equal to 7 wt% relative to the hide mass in limed state, at an initial pH of 2.8. After six hours running time, the pH was raised through the addition of an activation agent (sodium carbonate (diluted 1 : 10), 35 °C, 1.9 wt%). The effective pH was brought to 5.0 during a running time of 3 hours, and then ran overnight on 5 min rotation at 2 rpm per hour. The tanned leathers were finally washed at room temperature, mechanically dewatered (sammied), and shaved to the desired thickness.

FTIR spectroscopy of zeolites

10 g of zeolite was suspended in 50 ml of an aqueous acid–salt formulation (12.4% formic acid, 3.3% sulfuric acid, 28.1% sodium chloride) and stirred for 15 minutes. The suspension was passed through a 0.45 µm syringe filter. The clear liquid filtrate was collected and dried for 48 hours in an oven (Abinghurst, UK) at 105 °C. pH adjustment to pH 5.5 was achieved using 50% NaOH prior to drying at 120 °C. All infrared (IR) spectroscopy experiments were carried out using a Fourier transform (FT) IR spectrometer (PerkinElmer, Spectrum 65, Pike Miracle ZnSe ATR adapter). All experiments were carried out at 20.0 ± 1.0 °C, over the 600–4000 cm^{-1} wavenumber range; all spectra are averaged over 8 scans.

Sample digestion

Sample digestion was conducted in accordance with ISO 12914:2012. Approximately 0.2 g sections were cut from fully wet, tanned bovine hide, or 0.1 g of zeolite powder, were dried

in an oven (Abinghurst, UK) at 40 °C overnight. The dried samples were weighed and sealed into individual PTFE pressure vessels (CEM, USA) containing 8 ml aqua regia (1 : 3 molar ratio 68% nitric acid : 37% hydrochloric acid, Fisher Scientific) and 2 ml type I ultrapure water. The sealed pressure vessels were placed into a laboratory microwave oven (MARS6, CEM, USA) and were heated from room temperature to 180 °C in 10 minutes, maintained at 180 °C for 20 minutes, and cooled to 80 °C in 10 minutes. The pressurised samples were left to cool to room temperature naturally. The leather digests were diluted by a factor of 25 into a 250 ml volumetric flask using type I ultrapure water (Merek Millipore, Direct Q5, Germany).

Al(III) & Si(IV) concentration in aqueous solution

The Al(III) & Si(IV) contents of the dissolved zeolites were measured using inductively coupled plasma optical emission spectroscopy (ICP-OES) (Thermofisher Scientific, iCAP 6300, iTEVA software version 2.8.0.89). All measurements were made with respect to the 396.152 nm and 251.611 nm wavelengths for Al(III) and Si(IV) respectively using: a measurement time of 15 seconds, a stabilisation time of five seconds and a sample flush time of five seconds. The instrument pump rates were 100 rpm and 50 rpm for sample flushing, and analysis respectively; the radio frequency power was 1150 W; the auxiliary and nebuliser Ar gas flows were 0.5 and 0.7 l min^{-1} respectively. Calibration was achieved using solutions of known aluminium and silicon concentration over the 0–100 mg l^{-1} range. Mathematical conversions were used for the reporting of mineral oxide concentrations: $2Cr \rightarrow Cr_2O_3$: 1.46, $2Al \rightarrow Al_2O_3$: 1.89, $Si \rightarrow SiO_2$: 2.14, $12Al$ & $12Si \rightarrow Na_{12}Al_{12}Si_{12}O_{48}$: 2.58. The values for Cr were obtained from literature.[23]

Hydrothermal stability

The hydrothermal stability of the wet, tanned substrates was analysed using differential scanning calorimetry (Mettler Toledo, DSC 2, STARe software version 14). Samples approximately 25 mm × 25 mm were submersed in type I ultrapure water and sonicated (Dawe Sonicleaner) for 15 minutes. 5–10 mg specimens were taken from the substrate using a leather punch (Rolson) and placed into 40 μl aluminium pans hermetically sealed with aluminium lids (Mettler Toledo). The samples were heated from 40 °C to 100 °C at a heating rate of 5 °C min^{-1}.

Scanning electron microscopy and energy dispersive X-rays analysis

Scanning Electron Microscopy was conducted with a Tescan Vega 3, software version 4.2.34.1, 15 kV and a working distance of 15 mm. Energy dispersive X-ray analysis was also conducted with the above instrument and conditions using an Oxford Instruments Max-80 X-ray spectrometer attachment, AZTEC software, version 4.1. Elemental data was acquired over 90 seconds exposure intervals. Samples were prepared by dehydrating in acetone for 60 minutes followed by an exchange of fresh acetone for a further 20 minutes. The dehydrated

samples were dried at 20 °C for 60 minutes. The dried samples were submersed in liquid camphene at 50 °C overnight. Excess camphene was decanted, and the sample was frozen at −20 °C for 60 minutes. The sample was then cut with a razor blade and mounted on an imaging platform using an adhesive carbon pad (Agar Scientific, UK). A 15 nm gold coating was applied using a Quorum Q150R ES+.

NMR spectroscopy

^{27}Al magic-angle spinning (MAS) NMR measurements were performed on dried ground (<2 mm particle size) leather samples using a Bruker Avance III HD spectrometer operating at a ^{1}H Larmor frequency of 700 MHz. Samples were packed into 3.2 mm outer diameter rotors and spun at a MAS frequency of 18 kHz. The experimental time for each spectrum was 51 minutes.

SAXS procedures

SAXS measurements were performed on beamline 23A1 at the National Synchrotron Radiation Research Centre (NSRRC) in Hsinchu, Taiwan. Samples were cut into the size of 5 mm × 5 mm × 3 mm ($L \times W \times H$), loaded onto the holder and sealed in polyimide film to maintain the hydration level. Samples were exposed to the X-ray beam with an energy of 15 keV perpendicular to the surface. Scattered radiation was collected using a Pilatus 1 M detector located at a distance of 2.602 m from the sample. Data analysis for D-period, diffraction peak intensity and ratio were carried out following methods published elsewhere.[24,25]

Zeta potential procedure

Samples were dried in air and cut with a 12.7 mm diameter circular cutter and mounted to a Surpass electrokinetic analyzer (Anton Paar, Graz, Austria). A 10 mM solution of KCl, adjusted to pH 9.8 with KOH, was pumped through the sample. The electrolyte composition was varied by titrating with 100 mM HCl, and the pump pressure gradient varied stepwise from 0–300 mbar. The pressure and streaming current differentials were measured across the sample compartment. The Zeta potential (ζ) was calculated using the Helmholtz–Smoluchowsky relationship, eqn (1), where: the viscosity of the electrolyte solution (η), the dielectric constant of the electrolyte solution ($\varepsilon \cdot \varepsilon_0$), sample area ($A$), gap height ($l$), streaming current ($I$) and pressure ($p$) were considered. Samples were measured in duplicate.

$$\zeta = \frac{dI}{dp} \cdot \frac{\eta}{\varepsilon \cdot \varepsilon_0} \cdot \frac{l}{A} \qquad (1)$$

Green metrics

The mass uptake, quoted as percentage uptake, is calculated as the mass of offered zeolite based on the offered weight of zeolite product composition, considering waters of crystallisation, residual moisture and other components. This is expressed as per unit dry mass of the offered lime splits

material, assuming a 69% water content giving a theorical maximum zeolite content on dry weight.

The wastewater assessment is characterised by water consumption, chemical oxygen demand (COD), biological oxygen demand (BOD), total dissolved solids (TDS), total suspended solids (TSS) and metal salt concentrations. These are all measured according to current wastewater standards. The values obtained have been converted to per ton of raw hides mass, based on experimentally derived mass of 56% limed pelt per ton of raw hide, due to the splitting of hides. The conversion factor is used for calculating the wastewater amounts and freight per ton of raw hide. The biodegradability of tanned collagen fibres in process effluents was tested in accordance to ISO 20136:2017. To simulate the tanned fibre component of a process effluent, zeolite-tanned collagen was shredded and suspended in the test medium.

Results and discussion

Explanation of the application chemistry

Tanning of animal hides can be achieved *via* aqueous processing in drum vessels using a range of agents to stop the putrefaction process. Commonly, chromium(III) sulphate, glutaraldehyde, or polyphenolic plant extracts are used under acidic conditions which disperse, penetrate, and fix to the hide material. In this work, zeolites have been studied under comparable conditions to further understand the dispersion and transport chemistry within this context. The application of zeolite occurs over three processing stages: dispersion of the tanning agent, transport into the collagen matrix, zeolite restructure during activation. The pH profile demonstrating the reversibility of the dispersion during acid hydrolysis and the restructuring during activation can be found in the ESI Fig. S1.†

The infrared (IR) spectra of the dried dissolved solids recovered from the acid hydrolysis of the supplied zeolite are shown in Fig. 1 and have been used to infer an implicit structural fingerprint and locate differences in zeolite structure during the tanning process. A peak table can be found in the ESI Table S1.† The most prominent peaks at 1300 cm^{-1} (Al–O or Si–O stretching) 810 cm^{-1} (Al–O–Si or Si–O–Si bridges), 670 cm^{-1} (Al – O bending) appear to be unaffected by hydrolysis and activation.[26–29] However, the peak at 980 cm^{-1} (Si–O bonding) (ZL-P) broadens and shifts to 1100 cm^{-1} (ZL-A), which suggests the Si–O matrix is being significantly broken down. The limited changes in Al–O vibrations suggests this process is not simply the shortening of the NaAlSiO network.[26] The regeneration of the peak sharpness and shift back to 980 cm^{-1} (ZL-B) during activation suggests reformation of a Si–O network, however, it is not known if this is equivalent to the initial structure. The IR peaks in the 1750 cm^{-1}, 1400 cm^{-1} range relate to resonances originating from carboxylic acids as part of the zeolite composition.

^{27}Al Magic Angle Spinning (MAS) Nuclear Magnetic Resonance (NMR) spectra was used to probe the Al environ-
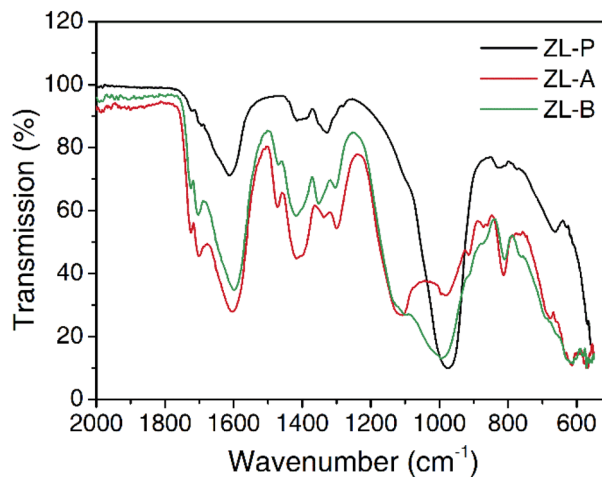

Fig. 1 IR Spectra of the dried dissolved solids recovered from a zeolite suspension: as supplied (ZL-P), after acid hydrolysis (ZL-A), after activation (ZL-B).

ment within the tanned collagen matrix, the spectra of which can be seen in Fig. 2. Aluminium salt tannages are commonplace for some specific leather end uses and have been used as individual tanning agents or in combination with polyphenolic tannins since prehistoric times.[1] Application of salts including potassium aluminium sulfate, aluminium sulfate, aluminium triformate result in retention of the inherent six-coordinate octahedral structure associated with the Al^{3+} ion which can be seen in Fig. 2 (COL-ALF) at 5 ppm. This shift is also consistent with chemical shift values for aluminium triformate
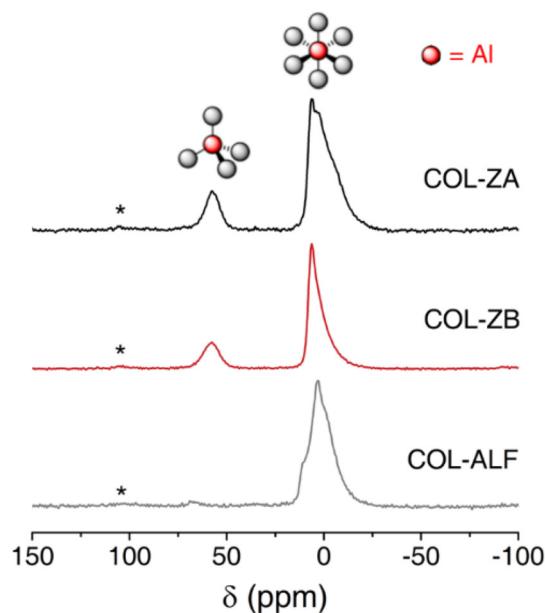

Fig. 2 ^{27}Al MAS NMR spectra for leather samples: zeolite-tanned pre-activation (COL-ZA), zeolite-tanned post-activation (COL-ZB) and aluminium triformate-tanned (COL-ALF) In each spectrum the asterisk denotes a spinning sideband.

from the literature.[30] Multiple unresolved signals are present, suggesting that there are several octahedral Al environments in this sample, which is not surprising considering the presence of chloride, sulphate and formate anions used as part of the overall tanning process.

The ^{27}Al MAS NMR spectrum for the aluminium triformate sample is distinct from the leather samples tanned with zeolite in that it lacks the resonances associated with tetrahedral four-co-ordinate species.[31] The ^{27}Al MAS NMR spectrum for the zeolite tanned leather sample before activation (Fig. 2, COL-ZA) shows two main features centred at 5 and 58 ppm. These shifts are consistent with six- and four-coordinate Al species, respectively, when the Al is in an oxide environment.[31] In this spectrum, the 5 ppm resonance is broadened and shows evidence of unresolved features, which suggests a range of environments are present, possibly from the presence of sulfate, chloride and formate interactions.

The ^{27}Al MAS NMR spectrum for the zeolite tanned leather sample after activation sample (Fig. 2, COL-ZB) is very similar to the pre-activation sample. However, the 5 ppm resonance is noticeably narrower, suggesting the Al species contributing to this resonance are in more similar environments. Given the anions contributing to the resonances in Fig. 2, COL-ZA, are also present post-activation, the sharpening of the 5 ppm resonance is likely to be due to the pH increases shifting the Al binding equilibrium in favour of forming an Al–O network.[31] The evidence in Fig. 2 supports the argument for the existence of multiple complex Al environments within zeolite-tanned leather beyond the recognised 6-coordinate environment observed by tanning with aluminium salts. The presence of 4-coordinate Al relates to aluminate anions, which are inherent to the zeolite structure, suggests larger, significant, aluminate macrostructures exist.

Table 1 lists the elemental compositions of animal hide tanned with either: zeolite, aluminium triformate, or 33% basic chromium sulfate (BCS). Where zeolite has been used, it is clear the concentrations of aluminium and silicon are equal suggesting equivalent dispersion, transport and restructuring of the aluminate and silicate components into an aluminosilicate structure. Cross-referencing this information with the evidence in Fig. 2 suggests the presence of larger aluminosilicate macrostructures.

The combination of the analyses outlined above confirms the method of application acts as a reversible pH-controlled breakdown, transport, and deposit mechanism for zeolites into fibrous collagen matrices. The administration of zeolites

can be achieved under conditions similar to other tanning chemistries adopted by the leather industry without the need for further specialist equipment or extended process time-lines.[1] The resulting leather material is stabilised against putrefaction and resistant to humid heat comparably to other commonly used stabilising agents.

Characterisation of the material

Thus far, the presence of the tanning agent is confirmed, however, the effect of the zeolite modification on the material properties and collagen structure have not been discussed. The effect and interaction mechanism of the stabiliser on the collagen fibre structure is unique to the agent used.[32] By understanding the interaction mechanism of zeolite in this context, further exploitation of the tanned material can be achieved.

The SAXS profile of the pickled bovine hide presented in Fig. 3A resembles those of materials from previous studies[33,34] showing the characteristic molecular arrangement of collagen in native fibrils. When treated with chromium(III) sulfate (CS) (COL-Cr), the known changes in peak intensities and positions are confirmed.[35,36] The 3rd order peak diminishes while the others increase relatively. The peaks also see shifts towards
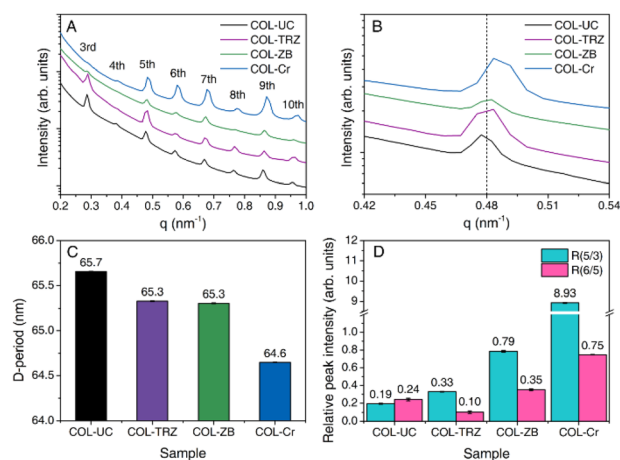
Fig. 3 *Ex situ* SAXS data comparing the hide materials with different stabilising treatments (A). *Ex situ* SAXS data focused on the 5th order peak (B). Changes in D-period of tanned hide collagen (C). Relative intensities of the 5th to 3rd order peaks ($R_{5/3}$) (BLUE), and of the 6th to 5th order peaks ($R_{6/5}$) (RED) of tanned hide collagen (D). Pickled hide (COL-UC), zeolite (COL-ZB), chromium(III) sulfate (COL-Cr) and triazine (COL-TRZ).

Table 1 The elemental compositions of animal hide tanned with a range of agents

	Tanning agent			
	Zeolite (mg kg^{-1})		Al triformate (mg kg^{-1})	BCS (mg kg^{-1})[17]
Elemental content	14 800 (±370) (Al)	14 900 (±1330) (Si)	14 400 (±310) (Al)	>18 000 (±1000) (Cr)
Oxide content (calculated)	28 000 (±700) (Al_2O_3)	32 000 (±2800) (SiO_2)	27 200 (±590) (Al_2O_3)	>26 300 (±1460) (Cr_2O_3)
Zeolite content (calculated)	76 600 (±8750) ($Na_{12}Al_{12}Si_{12}O_{48}$)			

higher q values indicating a smaller D-period between collagen molecules, as shown in Fig. 3B and C. It suggests a significant covalent binding of Cr(III) species to collagen, thereby interrupting the electron density contrast within the collagen matrix to result in this well-known change. However, using a triazine-based organic crosslinker (COL-TRZ) leads to minor changes in peak intensities, probably due to the absence of metallic species to enhance the contrast.[37] The zeolite tanning (with activation) (COL-ZB) behaves in between the two: it alters the peak intensities and positions only moderately. The calculations of the relative peak intensities of the 3rd and 5th order peaks ($R_{5/3}$) show a clear difference (Fig. 3D). Considering its equivalently high uptake as the CS-tanned samples (Table 1), one may propose that: while the zeolite forms covalent bonds to collagen to give the peak intensity changes, a considerable amount of zeolite is bound to collagen either *via* electrostatic interactions or hydrogen bonding. Additionally, the 6th to 5th order peak ratio indicates the hydration level of the collagen molecules, showing a slight increase when the hide is tanned with zeolite. On the contrary, the Cr(III) species give a much larger increase in the ratio indicating a stronger dehydration effect, whereas the organic triazine crosslinker gives a lower $R_{6/5}$, suggesting a more hydrated collagen matrix.[34] This observation highlights the metallic-like behaviour of the zeolite as Cr(III) which binds to water molecules surrounding the collagen molecule, leading to moderate dehydration effect.[32,33]

The concentrations of both the aluminium and silicon components are comparable with the concentrations observed in aluminium triformate-tanned and chromium(III)-tanned leather. This suggests the quantities of the zeolite stabilising agent needed to affect the hydrothermal stability successfully transfer into the fibrous collagen matrix.[23] However, the observation of the appropriate concentration of stabilising agent is not sufficient to confirm the strength of the stabilisation effect, therefore, the changes in denaturation resistance need to be explored, as shown in Table 2.[38]

Calorimetry data in Table 2 confirms zeolite not only increases the denaturation resistance of raw collagen, but also significantly changes the denaturation enthalpy in line with other established stabilising agents. Although the change in

resistance achieved using zeolite is not as pronounced as with chromium(III) sulfate, the change is sufficient to confirm zeolite stabilises collagen to an extent which is useful in a range of applications. Zeolite shows the most significant reduction in denaturation enthalpy of all the stabilising agents considered, which further supports the idea of a change in the collagen stability.[1] An increase in denaturation temperature directly correlates to an increase in the Gibbs free energy of the transition which can be a consequence of the stabilisation effect impacting on the enthalpy or entropy of denaturation.[1,5] Work by Weir has shown Chromium(III) stabilising agents predominantly stabilise by increasing the enthalpic component meaning there is a greater barrier to the denaturation process.[5] In contrast, all other stabilisers increase the denaturation free energy by lowering the entropic component, which can be considered an increase in steric hindrance that impedes collagen uncoiling during denaturation.[5] The significant reduction in denaturation enthalpy due to zeolite tanning implies denaturation resistance changes are accounted for by a reduction in system entropy. The ordering effect of the zeolite tanning correlates with the collagen dehydration observed by SAXS thus suggesting a relationship between steric hinderance, collagen hydration and denaturation temperature.[42]

All proteins exhibit an isoelectric point (IEP) which is dependent on the ratio of positively and negatively charged side-chain groups.[43] The IEP therefore indicates the pH where the transition between positive and negative surface charge occurs and is a useful indicator of material characteristics when considering further chemical modification. Compatibility with other chemicals with a surface charge, interaction with water and inherent collagen structure are all impacted by processing pH in relation to the IEP.[43] The IEP of a range of tanned collagen materials are presented in Table 3, which highlights how differently each stabilising agent can affect the collagen structure. The zeolite-tanned collagen IEP was derived from zeta potential measurements, whereas for other materials, the data was sourced from academic literature.[44]

Within collagen, the amino acids that significantly contribute to the IEP are: aspartic acid, glutamic acid, lysine, histidine and arginine, which result in an IEP of 7.4.[43] If the collagen has undergone alkaline treatment and temporarily stabilised in an acidic pickle formula, the IEP is lowered to 5.4 due to the conversion of asparagine and glutamine residues to aspartic and glutamic acid residues respectively under alkaline con-

Table 2 The denaturation onset temperature and enthalpies of bovine hide tanned with a range of tanning agents

Tanning agent	Onset temp (°C)	Enthalpy of denaturation (J g^{-1})
Zeolite	69 ± 7	15 ± 5
Aluminium triformate	68 ± 7	22 ± 3
Chromium(III) sulfate	110 ± 5 (ref. 39)	52 ± 2 (ref. 39)
Hydrolysable polyphenolics	75 ± 10 (ref. 39 and 40)	27 ± 3 (ref. 39 and 40)
Triazine	75 ± 2	19 ± 2
Glutaraldehyde	78 ± 3 (ref. 41)	36 ± 6 (ref. 42)
Pickled collagen	60 ± 5 (ref. 40)	49 ± 3 (ref. 40)
Raw collagen	50 ± 3 (ref. 39)	55 ± 3 (ref. 39)

Table 3 Isoelectric point of bovine hide modified by a range of tanning agents

Tanning agent	Isoelectric point
Raw collagen	7.4 (ref. 43)
Pickled collagen	5.4 (ref. 44)
Cr(III) or Al(III) salt	7.8 ± 0.5 (ref. 44)
Polyphenolic	4.4 ± 0.2 (ref. 44)
Glutaraldehyde	4.8 (ref. 44)
Triazine	4.5 (ref. 44)
Zeolite	3.9 ± 0.1

ditions.[45] Tanning with cationic Al(III) or Cr(III) salts results in interactions with negatively charged collagen sidechain groups (aspartate, glutamate), which leads to cationic charges overall at these reaction sites thus increasing the IEP to values near to that of raw collagen.[1] In contrast, the addition of zeolite results in the lowering of the IEP to 3.9. Despite the zeolite also being aluminium-containing, zeolites are known to have significantly anionic and highly porous structures.[46] Upon interaction with the collagen matrix, the ratio of cationic to anionic charges is considerably shifted in favour of being anionic. This observation is opposite to what is observed with Al(III) salts thus highlighting the inherently different aluminium environment, which correlates with the NMR analysis in Fig. 2 confirming the presence 4-coordinate aluminate structures. This suggests the anionic aluminate, silicate and aluminosilicate species are the major contributing species to the collagen stabilisation effect, whereas the cationic 6-coordinate Al(III) species are dominant in Al(III) salt tanning.

The binding mechanism between fibrous hide collagen and zeolite has been investigated with SAXS analysis on which observes the zeolite's effect on the nanoscale. The impact of the binding mechanism on the macroscale can be clearly seen by comparing the fibre structure of zeolite tanned against pickled bovine hides *via* SEM as shown in Fig. 4. The significant differences in fibre separation and gaps between fibre bundles vastly improves the physical properties of the resulting leather material allowing for a wide range of applications where strength and flexibility are required.[47] Without this fibre structure modification, the resulting leather material would be brittle and inflexible.[47]

The Energy Dispersive X-ray (EDX) line scans for the cross-sections of zeolite-tanned bovine hides are listed in the ESI (Fig. S2B†) and show the relative variance in Al and Si from grain (right) to flesh (left). The zeolite-tanned leather showed comparable Al and Si signal intensity across the whole cross-section suggesting Al and Si move in unison throughout the substrate. When compared with the EDX profiles of pickled collagen and aluminium salt-tanned leather, the Al and Si signals are not similar as shown in the ESI (Fig. S2C†). The EDX profile in Fig. S2B† also suggests the concentration of Al and Si are slightly lower in the centre compared to the substrate surfaces but this difference is regarded as insignificant.

In addition to the line scans reported in the ESI,† the secondary electron (SE) micrograph and corresponding 2D EDX maps in Fig. 5 also confirm the coincidence of Al and Si. This observation, combined with Fig. 2 and Table 1 converges on the notion of a significant presence of aluminosilicates dispersed throughout the collagen fibre structure. Separately, the micrograph in Fig. 5 lacks evidence of Al & Si particulates (>1 μm) despite the EDX maps clearly reporting the elemental presence. This suggests the structure of the Al and Si containing species is sub-micron and in significant contact with the collagen fibre matrix. This phenomenon is also observed in Cr(III) tanned leather where particular deposit of the stabilising agent is not observed.[48]

The combination of SAXS analyses, SEM observation and the marked changes in IEP highlight how zeolites bind to collagen and impact on the resulting material properties. Despite containing Al(III), there is support from several aspects that the zeolite stabilisation effect is noticeably different compared to
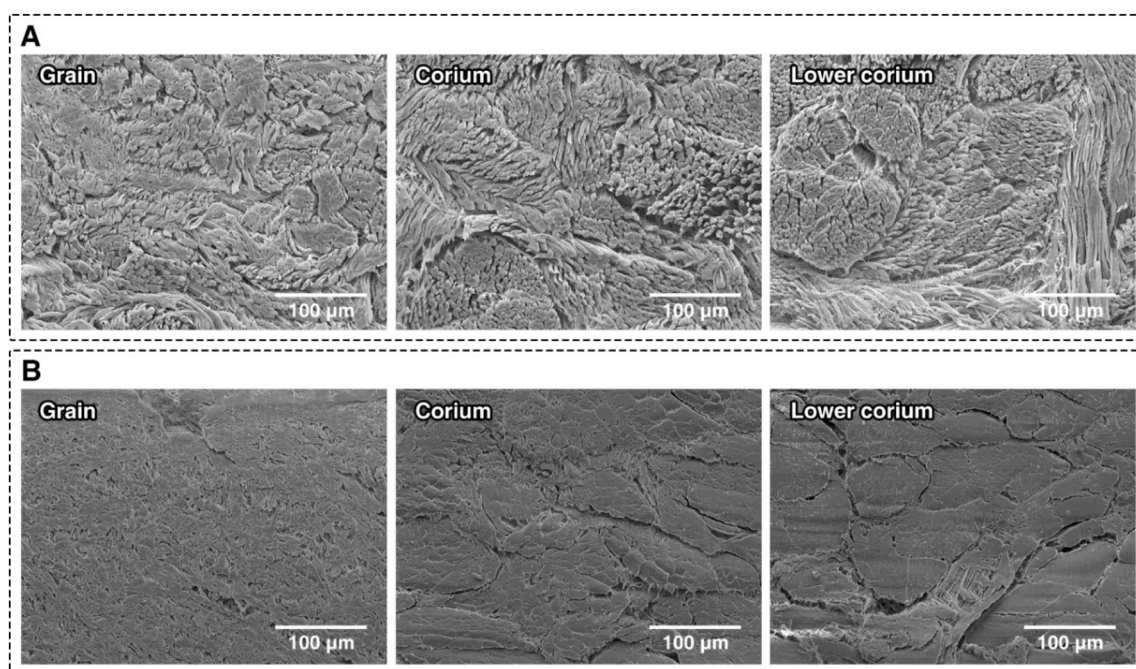

Fig. 4 Micrographs comparing the fibre structure of zeolite-tanned (A) and pickled bovine hide (B): the images correlate to the: grain (left), mid-corium (middle), and lower corium (right).
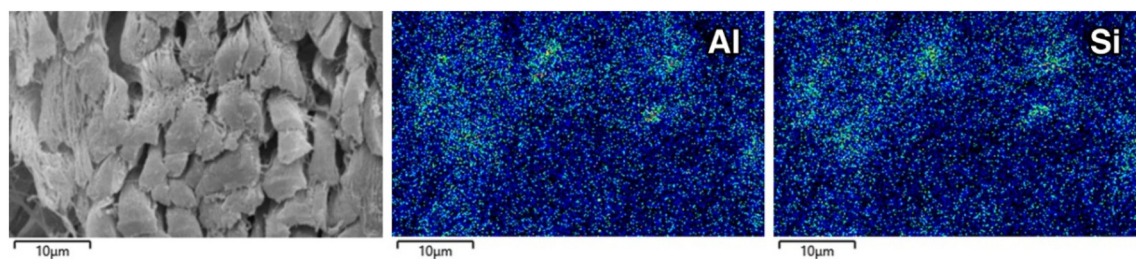
Fig. 5 Secondary electron micrograph of zeolite-tanned bovine hide (left) with corresponding Al (centre) and Si (right) 2D EDX maps.

Al(III) salts such as aluminium triformate or aluminium sulfate. Aluminum(III) salts tan *via* electrostatic interactions with a significant ionic character, which is reversible, and does little to improve the macroscopic physical properties through fibre separation.[49] Zeolite tanning is noticeably more non-ionic in character and permanent in-line with a tanning agent with characteristics of both Cr(III) salts and organic cross-linkers with a clear impact on fibre separation.

Applications

Collagenic materials are versatile with a wide range of possible applications including: medical, food and general material uses. The largest sector for the use of collagenic materials is the leather industry with approximately 17 billion m² of leather produced annually being made into shoes, bags, clothing and seat covers.[50,51] The use of zeolite stabilisers has been successfully patented and industrial scale production is in place.[52] The application of zeolite stabilisers produces an intrinsically white tactile leather material from non-toxic and abundant chemistry, which is now being adapted for a range of end-uses including compostable shoes[53,54] and bags.[55] Although leather production is the single biggest application of collagenic materials, the benign nature of zeolite tanning provides potential to diversify into non-leather materials including medical and food applications.

Green metrics relevant for applications at larger scale

To show the environmental implications of a zeolite tanning process, a feasibility study has been conducted which evaluates the mass uptake, water usage, and biodegradability of process effluents. Reference comparisons are made to industrial best available technology (BAT); the lab-scale is defined as 35 kg (2 hides) whereas the pilot-scale is defined as 550 kg (30 hides). As zeolite is a combination of the elements silicon, aluminium and oxygen, analysing the exact total amount of

aluminosilicate is challenging. It has been repeatedly confirmed in Table 1 and Fig. 4 and 5, that Al and Si are coincident and present in equivalent quantities, therefore, the amount of zeolite present is based on the amount of Al analysed and used as an indicator of the total amount taken up in the process, thus defining the mass uptake of zeolite tanning. The same approach can be made with silicon, as is shown in Tables 1 and 4, which shows similar uptake amounts at the lab-scale. Silicon analyses are not performed at pilot scale as it requires more extensive testing and less reliable, thus making this in practice not applicable. Upscaling effects are expected and observed, which increases the overall uptake percentage to over 90%. These upscaling effects can be attributed to increases in mechanical action on the hides, leading to improvement in the penetration and eventually uptake of the tanning chemistry.

The assessment of tanning process wastewater is summarised in Table 5 and Fig. 6 and is compared to industry best practice.[56] The overall water consumption is slightly higher compared to the industry best standard, whereas the pH is typically higher making it easier to process.[56] The lack of chromium present in the wastewater and Al values of 0.2 kg t⁻¹ is an important aspect as this makes the processing easier. In standard chromium(III)–salt tanning practices, the wastewater streams need to be kept separated to limit chromium pollution.[56] Wastewater streams coming from zeolite tanning can be mixed without limitation as aluminium does not have to be specifically treated separately.

Table 5 Zeolite tanning water consumption compared to industry best practice

	Zeolite tanning	Industry best practice
Water consumption (m³ t⁻¹)	0.7–0.9	0.5–0.7
pH	4.8–5.5	4.0–4.4

Table 4 Mass uptake of tanning chemistry at lab and pilot scale

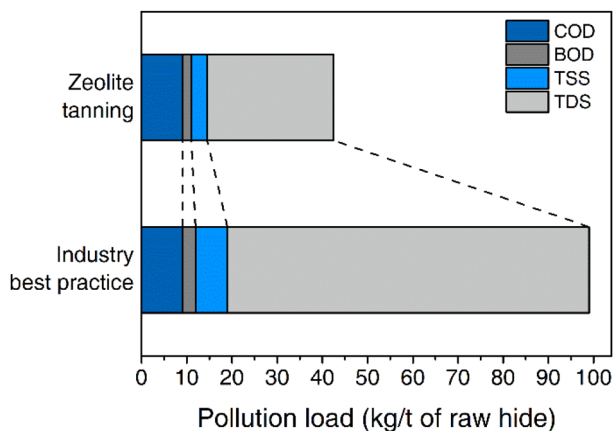| Application scale	Application offer (%)	Element	Content theoretical (mg kg⁻¹)	Content measured (mg kg⁻¹)	Zeolite content (g kg⁻¹)	Uptake %
Lab	6	Al	20 900	14 800 (±370)	70	71
		Si	21 290	14 900 (±1330)	70	70
Pilot	7	Al	24 390	22 080 (±4030)	104	91

Fig. 6 Pollution load of zeolite tanning wastewater compared to industry best practice.

Table 6 Relative and absolute biodegradability of leather waste streams with a range of tanning agents

Tanning agent	Absolute biodegradability (%)	Relative biodegradability (%)
Collagen (not tanned)	91.9	100
Zeolite	75.0	81.6
Cr(III) salt	3.8	4.1
Glutaraldehyde	22.1	24.1

During leather production, tanned collagen fibres enter the process effluents and present a waste stream that needs consideration. The biodegradability of shredded tanned-collagen fibres in the process effluent has been compared to other tanning agents in the industry by bacterial degradation pathways according to ISO 20136:2017, as listed in Table 6. Absolute biodegradability relates to the mass of the sample used, whereas relative biodegradability is relative to the collagen sample tested.

From Table 6, it is clear the zeolite-tanned collagen fibres shows a high biodegradability in these aqueous conditions, especially compared to Cr(III)-tanned. With the zeolite-tanned intermediate leather, there is the option for creating leather that is durable, long lasting, and biodegradable without possibly toxic elements. The industry is already exploring opportunities by working on compostable leather based on zeolite tanning, thus bringing leather closer towards a circular economic future.

Conclusions

The mechanism for the tanning of a sustainable leather material using zeolites has been demonstrated. NMR data and elemental analysis have revealed the activated zeolites form an aluminosilicate network structure covering the collagen fibres, which stabilises the protein fibre structure. SAXS analysis has highlighted the characteristics of the binding mechanism are

between an organic cross-linker and a metal salt in terms of interactions and collagen dehydration. Zeolite-tanning sets the precedent for the future of leather materials with clear environmental, sustainability and material benefits. Industrial scale has been achieved and a range of products are being made from this material, which clearly illustrates its position in the circular economy with scope to diversify into medical and food applications.

Data availability

All data underpinning this publication are openly available from the University of Northampton Research Explorer at **https://doi.org/10.24339/3ffe0d06-04ba-415d-82c7-27b15f93c3eb**.

For the purpose of open access, the authors have applied a Creative Commons Attribution (CC BY) licence to any Author Accepted Manuscript version arising from this submission.

Author contributions

W. R. W.: Validation, visualisation, supervision; S. J. D.: Writing – original draft, data curation, formal analysis, investigation; W. E. H.: Conceptualisation, supervision, writing – original draft; D. J. A. V.-B.: Project administration, validation; S. P.: Methodology, resources, funding acquisition; Y. Z.: Formal analysis, investigation, writing – review & editing.

Conflicts of interest

The authors state there are no conflicts of interest to declare.

References

1 A. D. Covington and W. R. Wise, *Tanning Chemistry: The Science of Leather*, Cambridge, 2nd edn, 2020, ch. 10, pp. 195–203.
2 S. S. Kremen and R. M. Loller, *J. Am. Leather Chem. Assoc.*, 1951, **46**, 34.
3 C. A. Miles, *J. Mol. Biol.*, 2005, **346**, 551.
4 A. D. Covington, R. A. Hancock and I. A. Innidis, *J. Soc. Leather Technol. Chem.*, 1989, **73**, 1.
5 C. Weir, *J. Am. Leather Chem. Assoc.*, 1949, **44**, 108.

6 G. George, *Industry Insight: Challenges of the Leather Supply Chain*, https://www.pergamena.net/blog/v3piynz4zg9ysu-box7b1r3zszwrfx8, (accessed 2nd March 2023).

7 F. Knapp, *Natur und Wesen der Gerberei und des leders*, J. G. Cotta, Jena, 1858.

8 A. D. Covington, *Tanning Chemistry: The Science of Leather*, Cambridge, 1st edn, 2009, ch. 11, pp. 204–258.

9 A. Marsal, *Soc. Leather Technol. Chem.*, 1999, **83**, 300.

10 K. Nakagawa, *Hikaku Kagaku*, 1999, **45**, 210.

11 A. D. Covington and R. L. Sykes, *J. Am. Leather Chem. Assoc.*, 1984, **79**, 72.

12 D. F. Shriver, P. W. Atkins and C. H. Langford, *Inorganic Chemistry*, Oxford University Press, Oxford, 2nd rev. edn, ch. 11, 1995, p. 457.

13 S. Narayanan, P. Tamizhdurai, V. L. Mangesh, C. Ragupathi, P. Santhana Krishnand and A. Ramesh, *RSC Adv.*, 2021, **11**, 250.

14 A. Petushkov, N. Ndiege, A. K. Salem and S. C. Larsen, *Adv. Mol. Toxicol.*, 2010, **4**, 223.

15 P. Zarrintaj, G. Mahmodi, S. Manouchehri, A. H. Mashhadzadeh, M. Khodadadi, M. Servatan, M. R. Ganjali, B. Azambre, S.-J. Kim, J. D. Ramsey, S. Habibzadeh, M. R. Saeb and M. Mozafari, *MedComm*, 2020, **1**, 5.

16 ZeoDet, *Zeolites for Detergents – As nature intended*. https://www.euzepa.eu/images/3.ZEODETbrochure.pdf, (accessed 2nd march 2023).

17 K. H. Munz, *J. Am. Leather Chem. Assoc.*, 2003, **98**, 159.

18 D. Faraji, A. Jahandideh, A. Asghari, A. Akbarzadeh and S. Hesaraki, *Arch. Razi Inst.*, 2019, **74**, 395.

19 P. Ciambelli, D. Sannino, B. Naviglio, A. M. Manna, V. Vaiano, G. Calvanese, G. Vietri and S. Gallo, *Stud. Surf. Sci. Catal.*, 2005, **155**, 189.

20 F. Chiardelli, N. Costantini and A. D. Covington, *J. Am. Leather Chem. Assoc.*, 2000, **95**, 125.

21 A. Bacardit, S. van der Burgh, J. Armengol and L. Ollé, *J. Cleaner Prod.*, 2014, **65**, 568–573.

22 C. Bagiran, D. Brendler and F. Wegener, *Eu. Pat* EP2574682A1, 2011.

23 Y. Zhang, B. W. Mansel, R. Naffa, S. Cheong, Y. Yao, G. Holmes, H.-L. Chen and S. Prabakar, *ACS Sustainable Chem. Eng.*, 2018, **6**, 7096.

24 Y. Zhang, T. Snow, A. J. Smith, G. Holmes and S. Prabakar, *Int. J. Biol. Macromol.*, 2019, **126**, 123.

25 Y. Zhang, J. Buchanan, R. Naffa, B. Mansel, C. Maidment, G. Holmes and S. Prabakar, *J. Synchrotron Radiat.*, 2020, **27**, 1376.

26 H. L. Jamieson, H. Yin, A. Walker, A. Khosravi and M. L. Lind, *Microporous Mesoporous Mater.*, 2015, **201**, 50.

27 M. W. Urban, *Vibrational Spectroscopy of Molecules and Macromolecules on Surfaces*, Wiley, New York, 1993.

28 T. Xia, W. D. Zhuang, X. Z. Cui, C. I. Zhao, X. M. Teng and X. W. Huang, *J. Rare Earths*, 2006, **24**, 141–144.

29 W. Mozgawa, M. Sitarz and M. Rokita, *J. Mol. Struct.*, 1999, **511–512**, 251.

30 J. H. Roque-Ruiz, E. A. Cabrera-Ontiveros, G. González-García and S. Y. Reyes-López, *Results Phys.*, 2016, **6**, 1096–1102.

31 M. L. Adams, *Speciation and measurement of aluminium in environmental systems*, PhD thesis, University of Canterbury, 1999.

32 Y. Zhang, B. Ingham, S. Cheong, N. Ariotti, R. D. Tilley, R. Naffa, G. Holmes, D. J. Clarke and S. Prabakar, *Ind. Eng. Chem. Res.*, 2018, **57**, 63.

33 Y. Zhang, B. W. Mansel, J. K. Buchanan, J. Su, Z. Zhang, G. Holmes and S. Prabakar, *J. Am. Leather Chem. Assoc.*, 2020, **115**, 373.

34 J. K. Buchanan, Y. Zhang, G. Holmes, A. D. Covington and S. Prabakar, *ChemistrySelect*, 2019, **4**, 14091.

35 Y. Zhang, B. W. Mansel, R. Naffa, S. Cheong, Y. Yao, G. Holmes, H.-L. Chen and S. Prabakar, *ACS Sustainable Chem. Eng.*, 2018, **6**, 7096.

36 Y. Zhang, M. Mehta, B. W. Mansel, H. W. Ng, Y. Liu, G. Holmes, E. C. Le Ru and S. Prabakar, *Biopolymers*, 2020, e23406.

37 X. Liu, Y. Wang, X. Wang, T. Han, W. Wang and H. Jiang, *Green Chem.*, 2022, **24**, 2179.

38 E. Onem, A. Yorgancioglu, H. A. Karavana and O. Yilmaz, *J. Therm. Anal. Calorim.*, 2017, **129**, 615.

39 A. Cucos, C. Gaidau, E. Badea and L. Miu, *Rev. Roum. Chim.*, 2015, **60**, 1093.

40 C. Carsote, E. Badea, L. Miu and G. Della Gatta, *J. Therm. Anal. Calorim.*, 2016, **124**, 1255.

41 A. Yorgancioglu, E. Onem, O. Yilmaz and H. A. Karavana, *Johnson Matthey Technol. Rev.*, 2022, **66**, 215.

42 C. A. Miles, N. C. Avery, V. V. Rodin and A. J. Bailey, *J. Mol. Biol.*, 2005, **346**, 551.

43 A. D. Covington and W. R. Wise, *Tanning Chemistry: The Science of Leather*, Cambridge, 2nd edn, 2020, ch. 1, pp. 1–31.

44 Y.-N. Wang, W. Huang, H. Zhang, L. Tian, J. Zhou and B. Shi, *J. Am. Leather Chem. Assoc.*, 2017, **112**, 224.

45 O. Menderes, A. D. Covington, E. R. Waite and A. C. T. van Duin, *J. Soc. Leather Technol. Chem.*, 1999, **354**, 1379.

46 C. J. Heard, L. Grajciar, F. Uhlík, M. Shamzhy, M. Opanasenko, J. Čejka and P. Nachtigall, *Adv. Mater.*, 2020, **32**, 2003264.

47 A. D. Covington and W. R. Wise, *Tanning Chemistry: The Science of Leather*, Cambridge, 2nd edn, 2020, ch. 6, pp. 157–179.

48 A. D. Covington and W. R. Wise, *Tanning Chemistry: The Science of Leather*, Cambridge, 2nd edn, 2020, ch. 17, pp. 462–496.

49 M. Komanowsky, *J. Am. Leather Chem. Assoc.*, 1989, **84**, 369.

50 Global Leather Goods Industry 2013–2018: Trend, Profit and Forecast Analysis, Lucintel.

51 A. Covington, *Chem. Soc. Rev.*, 1997, **26**, 111–126.

52 W. E. Hendriksen, D. J. A. Von Behr and P. J. Wilgenburg, *NL Pat* 2024455, 2019.

53 Nera Tanning, https://www.neratanning.com/news/puma-develops-biodegradable-resuede-sneaker-with-zeology-leather/, (Accessed 29th November 2022).

54 Nera Tanning, https://www.neratanning.com/news/the-very-first-chrome-free-leather-sneakers-in-the-us/ (Accessed 29th November 2022).

55 Nera Tanning, https://www.neratanning.com/news/collaboration-with-anya-hindmarch-for-game-changing-bag-collection/, (Accessed 29th November 2022).

56 M. Black, M. Canova, S. Rydin, B. Scalet, S. Roudier and L. Delgado Sancho, *Best Available Techniques (BAT) Reference Document for the Tanning of Hides and Skins: Industrial Emissions Directive 2010/75/EU:(Integrated Pollution Prevention and Control)*, Publications Office of the European Union, Luxembourg, 2013.